Journal of Optoelectronic and Biomedical Materials Vol. 12, No. 3, July - September 2020, p. 73 - 79

THEORETICAL INVESTIGATION OF A DOUBLE-RESONANCE PLASMONIC IN MULTILAYER STRUCTURE INTENDED FOR BIOMEDICAL DETECTION

A. SAOULI[a,*], C. SAOULI[b]
[a]*Department of electronics, Mentouri Brothers University of Constantine. Constantine, Algeria*
[b]*Department of chemistry, Mentouri Brothers University of Constantine. Constantine, Algeria*

The photo electronic devices based on surface plasmon resonance (SPR) phenomena have wide applications in the biomedical field. The biological environments to be detected are influenced by the SPR phenomenon, perhaps by the wavelength or the angle of incidence of resonance. In this work, the angular analysis of the phenomenon of double SPR in multilayer nanostructures is modeled by the transfer matrix method (T matrix). Consequently, we find that we can eliminate the error of simple SPR response and double SPR response based on the absolute deference response between the first SPR resonance and the second SPR double resonance.

(Received March 7, 2020; Accepted August 13, 2020)

Keywords : Double SPR phenomena, Multi layers nanostructures, T-matrix

1. Introduction

The effect of the surface plasmon (SPR) present in several domains in in recent years, in the detection of the DNA [1,2], waveguides to be applied in biosensor [3,4], therefore the detection of the bio-body [5]. In biomedicine [6,7], bio-analysis [8,9], optics [6,10] and solar energy [11]. Each application results in a specific structure, either continuous metallic nanostructures [3,10] or discrete such as finds spherical [6,11], cylindrical [6], cubic [6]. Indeed, scientific research in this new rich field is very active for it to integrate into industry. For example, in the biomedical field, there are several marketed instruments that operate on the basis of the SPR effect such as Biacore X, 3000, S51 and X100 of GE Healthcare company, Reichert SR7500DC and 4SPR of Reichert Technologies company, BI-SPR of Biosensing Instruments company, SensiQ of SensiQ Technologies company, Open SPR of Nicoya instrument company, Indicator-G research platform of Sensia company, BioNavis MP-SPR Navit family of products: MPSPR Navit200 OTSO, MP-SPR Navit210A VASA, MP-SPR Navit220ANAALI, and MP-SPR Navit420A ILVES of BioNavis company, BIOSUPLAR-6 of Analyticalm-Systems company [12].

The SPR effect is greater in noble metals whose imaginary part ε2 of the dielectric function ($\varepsilon = \varepsilon 1 + i \times \varepsilon 2$) is weak. An important consequence of this is that a TE polarized light beam will not cause an oscillation of the charges at the metal / dielectric interface. There will be no excitation of surface plasmons for this polarization. On the contrary, an evanescent TM wave arriving at the dielectric / metal interface will decompose in this latter medium into a transverse wave and another longitudinal one. This longitudinal component of the wave in the metal will then create a longitudinal vector potential which will be able to couple to the oscillations of density of surface charges or surface plasmons [13].

In this work we are interested in continuous structures based on thin full metallic layers. The surface plasmon resonance phenomenon is used for the detection, identification and quantification of molecules on the one hand and biophysical analyzes of biomolecular interactions on the other [12]. SPR has certain advantages in the field of biosensors, including ease of use, sensitivity and real-time measurements. There are two methods of detection, the angular

[*]Corresponding author: abdelali.saouli@lec-umc.org

interrogation (θ) which consists in supporting the angular position of the minimum reflectivity SPR at a wave length of incidence (λ) fixes, and the spectral interrogation that consists in supporting the spectral position (λ) of the minimum reflectivity SPR at an angle of incidence θ fixed. The study of angular response of the multi layers SPR detector based on the method of transfer matrices (T - matrix).

The rest of this paper is organized as follows. In Section II, present the implementation of the T -matrix in calculation SPR reflectivity of electromagnetic plane wave (TM). Section III, shows the result and discussion. Section V summarizes the contributions of this paper.

2. Physic-mathematical system presentation

The SPR sensor used in the configuration is composed of several layers fig. 1 and TM polarized light beam. There are a more complex method is therefore necessary to correctly describe the expected signal. So, in order to obtain a theoretical model of the SPR profile, a matrix is used for multibeam interference. For clarification, the following derivation is based on the work of Klein and Furtak [14].

We have the transition of the fields on the interface between the medium i and j and given by [14]:

$$\begin{pmatrix} E'_{li} \\ E'_{ri} \end{pmatrix} = \frac{1}{\tau_{ij}} \begin{pmatrix} 1 & \rho_{ij} \\ \rho_{ij} & 1 \end{pmatrix} \begin{pmatrix} E_{lj} \\ E_{lj} \end{pmatrix} \tag{1}$$

and:

$$E' = H_{ij} E \tag{2}$$

where H_{ij} is the matrix describing the transition of the fields on the interface between the media i and j and given by:

$$H_{ij} = \frac{1}{\tau_{ij}} \begin{pmatrix} 1 & \rho_{ij} \\ \rho_{ij} & 1 \end{pmatrix} \tag{3}$$

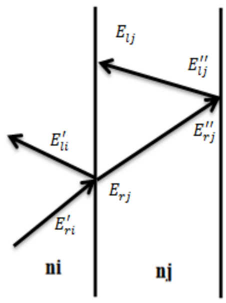

Fig. 1. Detailed model of the optical situation analyzed. The electric field (E'_{ri}) moves from left to right through the mediums characterized by their refractive indices ni and nj [14].

Also, if the incident wave is polarized p (TM mode), so that the field E is in the plane incidence, τ_{ij} and ρ_{ji} are given by[14]:

$$\tau_{ij} = \frac{2(n_i/n_j)}{1+b} \tag{4}$$

and:

$$\rho_{ji} = \frac{1-b}{1+b} \tag{5}$$

where:

$$b = \left(\frac{n_i}{n_j}\right)^2 \left(\frac{k_{z,j}}{k_{z,i}}\right) \tag{6}$$

where, ñi and ñj is the complex reactivity index of the medium i and j, and $k_{z,j}$ is the reciprocal wave number of the field E in the medium j.

As well, the transition of the fields through the medium j and given by [15]:

$$\begin{pmatrix} E_{lj} \\ E_{lj} \end{pmatrix} = \begin{pmatrix} e^{\beta j} & 0 \\ 0 & e^{-\beta j} \end{pmatrix} \begin{pmatrix} E_{li}^{"} \\ E_{ri}^{"} \end{pmatrix} \tag{7}$$

and:

$$E = L_j E^{"} \tag{8}$$

where L_j is the matrix for the transaction through the medium j using a phase factor $e^{\beta j}$ given by:

$$L_{j=} \begin{pmatrix} e^{\beta j} & 0 \\ 0 & e^{-\beta j} \end{pmatrix} \tag{9}$$

where $e^{\beta j}$ is given by [13]:

$$\beta j = \frac{2\pi}{\lambda} n_j d_j \cos\left(\theta_j\right) \tag{10}$$

Subsequently and by combining the matrices H and L of several layers, we obtain a total matrix, a complete stack of layers.

$$H_{12} L_{i2} H_{23} L_3 \cdots H_{ij} L_j \cdots H_{N-1,N} L_N = S_{1N} = \begin{pmatrix} S_{11} & S_{12} \\ S_{21} & S_{22} \end{pmatrix} \tag{11}$$

Finally, the reflectance of the stack is then given by [15]:

$$R = \left|\frac{S_{21}}{S_{11}}\right|^2 \tag{12}$$

Concerning boundary conditions at the interface, it's requiring continuity in the magnitude of the field. This continuity also imposes the relation between the dielectric constants [15]:

$$\frac{k_{z,j}}{k_{z,i}} = -\frac{\varepsilon_j}{\varepsilon_i} \tag{13}$$

$$k_{z,i}^2 = k_x^2 - k_0 \varepsilon_i \tag{14}$$

$$k_{z,j}^2 = k_x^2 - k_0\varepsilon \tag{15}$$

In the latter we conclude that the combination of these last three equations and the definition of the vacuum propagation vector k0 = ω / c give us the dispersion relation:

$$k_x = \frac{\omega}{c}\sqrt{\frac{\varepsilon_i\varepsilon_j}{\varepsilon_i + \varepsilon_j}} \tag{16}$$

However, it can be deduced that the angular frequency depends on the dielectric constant, and therefore the refractive index, as $\varepsilon = \tilde{n}^2$. This derivation is however fairly basic, because it is only valid for an interface with metal and dielectric.

3. Result and discussion

The first structure studied is shown in Fig. 2. We notice that there are three layers with complex refractive indexes n1, nm and n2, where nm is the refraction index of metal.

The metal used in this structure is Gold with refractive index nAU = 0.17-i*4.93 for wavelength of 780 (nm) [16].

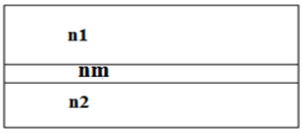

Fig. 2. Structure studied in three layers.

The reflectance curves as a function of the angle of incidence of the wave plane in TM mode and different values of n1 are presented in “Figs. 3”. It is noted that the SPR effect is present in all the reflectance curves with the optical parameters and the geometries presented in the figures (Fig. 3). For example, the SPR resonance is located at θSPR= 62.16 (deg) for n1=1.4 and in θSPR= 28.43 (deg) for n1=2.6 (Figs. 3).

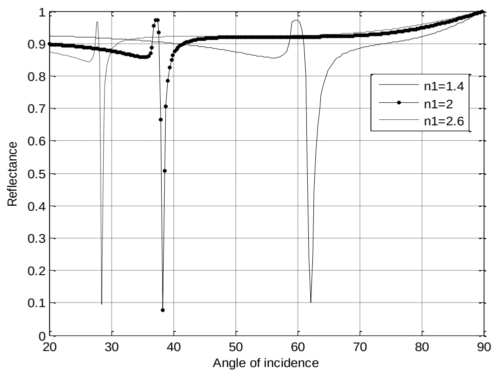

Fig. 3. Variation of the reflectance as a function of the angle of incidence and different values of n1: n2 = 1.2, λ= 780 [nm], dAu = 40 [nm].

Since it is that the SPR response of a biomedical detector structure is based on the detection of change in the SPR angle as a function of change in the optical properties of the biological medium studied (the refractive index) [12], It is assumed that the biological medium studied is positioned at top of the metal with a refractive index n1, The SPR response based on

Gold is presented in Fig. 4. We notice that the SPR angle decreases with the increase of n1, and for a change range of Δn1=2, the θSPR (SPR angle) registers a range of almost ΔθSPR=42 (deg), which gives us a good sensitivity to the detector structure studied.

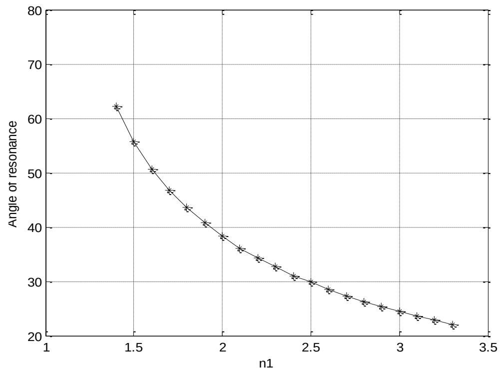

Fig. 4. Variation of the angle of resonance for the SPR as a function of n1: n2 = 1.4, λ= 780 [nm], dAu = 40 [nm].

The second structure studied is shown in Fig. 5. We notice that there are five layers with complex refractive indices n1, n2, n3, nm, where nm is the refractive index of the metal. The metal used in this structure is Gold with same refractive index of the first structure; there are two layers of metal with a thickness of 40 (nm) separated by a layer whose refraction index is n2 and thickness of 70 (nm).

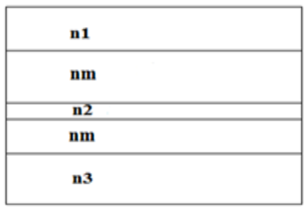

Fig. 5. Structure studied in five layers.

The curves of reflectance versus angle of incidence of wave plane in TM mode and for different n1 values of second structure (fig. 5) are shown in Fig. 6. We notice that the double SPR effect is present in all the reflectance curves with the optical parameters and geometries presented in the figures (Fig. 6). For example, the double SPR resonance is located in θSPR1=61.27 and θSPR2=75.98 (deg) for n1=1.4 with absolute difference of Δθ= 14.71 (deg) and in θSPR1=28.12 and θSPR2=31.63 (deg) for n1=1.4 with absolute difference of Δθ= 3.51 (deg) (Fig. 6).

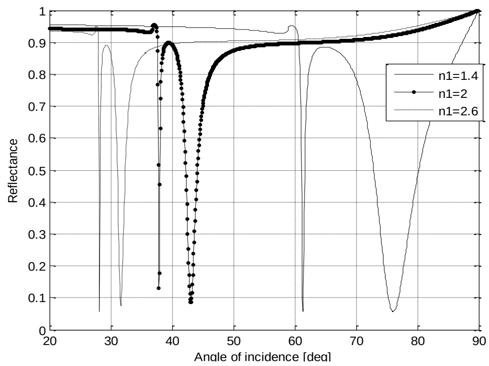

Fig.6. Variation of the reflectance as a function of the angle of incidence and different values of n1: n2 = 1, n3 = 1.2, λ= 780 [nm}, d2=70 [nm], dAu = 40 [nm].

The SPR response based on Gold of second structure is presented in Fig. 7.

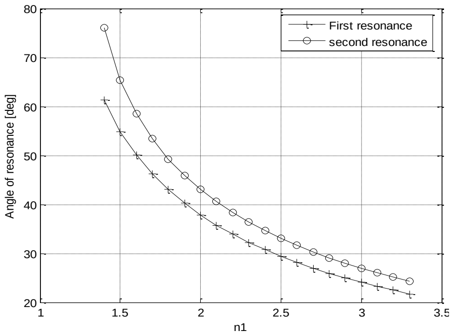

(a)

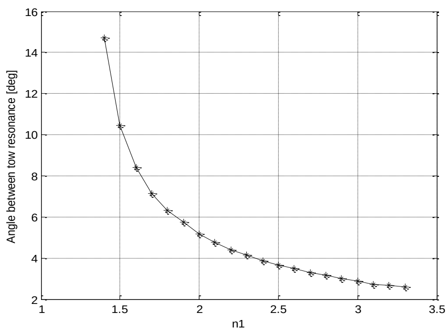

(b)

Fig. 7. Variation of the angle of resonance for the double SPR as a function of n1, a) for the first and second resonance, b) for the absolute different between first and second resonance: n2 = 1, n3 = 1.2, λ= 780 [nm}, d2=70 [nm], dAu = 40 [nm].

We note that the SPR response for the first resonance (Fig. 7.a) is almost the same shape of SPR response for the first structure of three layers and one SPR effect (Fig. 4), but SPR response for the second resonance (Fig. 7.a) register an offset of a positive value compared to the first SPR resonance. The positive offset between two SPR resonances in double SPR resonance of the second structure is shown in Fig. 7.b.

up to this level, there are four response curves: one for the first structure of a single SPR resonance (fig. 4), two for the second structure of a double SPR resonance (one for the first SPR resonance and other for the second SPR resonance) (fig. 7.a), and the last is the offset between the double resonance SPR of the second structure (fig. 7.b).The question that arises, what is the best response curve?

If we analyze at the error level, in each of the two structures we make an error (Error 1, Error 2), so we have:

$$\theta 1_{SPR}(n1) = \theta 10_{SPR}(n1) + Error1 \tag{17}$$

$$\theta 2_{SPR1}(n1) = \theta 20_{SPR1}(n1) + Error2 \tag{18}$$

$$\theta 2_{SPR2}(n1) = \theta 20_{SPR2}(n1) + Error2 \tag{19}$$

where: $\theta 1_{SPR}(n1)$ is the response curve of the first structure, and $\theta 2_{SPR1}(n1)$, $\theta 2_{SPR2}(n1)$ are the response curves of the second structure double SPR.

$\theta 10_{SPR}(n1)$ is the response curve of the first structure without error, and $\theta 20_{SPR1}(n1)$, $\theta 20_{SPR2}(n1)$ are the response curves of the second structure without error for double SPR.

Error1 and Error2 are the errors in the two structures (single and double SPR resonance respectively).

Sow, the response curves of the last ($\Delta\theta_{SPR12}(n1)$) is the offset between the double resonances SPR of the second structure calculate from absolute different of $\theta 2_{SPR1}(n1)$ and $\theta 2_{SPR2}(n1)$:

$$\Delta\theta_{SPR12}(n1) = \left|\theta 2_{SPR2}(n1) - \theta 2_{SPR1}(n1)\right| \tag{20}$$

$$\Delta\theta_{SPR12}(n1) = \left|\theta 20_{SPR2}(n1) + Error2 - \theta 20_{SPR1}(n1) - Error2\right| \tag{21}$$

$$\Delta\theta_{SPR12}(n1) = \left|\theta 20_{SPR2}(n1) - \theta 20_{SPR1}(n1)\right| \tag{22}$$

From this analysis we can say that the last response curve is the best answer due to the elimination of errors.

4. Conclusions

In this paper, we have presented the simulation of the response of a multilayer SPR detector structure. The work carried out concentrated on the part of the design of the structure and the response of the latter in the visible optical band in TM mode based on the semi-analytical method T-Matrix and the Matlab software. First, we carried out the design of the studied multilayer SPR structure; we proposed dimensions of the studied structure and adapted the optical properties of the layers with these dimensions to say the single and double SPR effect exists in the response of the studied structures, in reflection at the incidence angle.

The results of the simulation we obtained and the theoretical approach which led to it, show that we can eliminate the error in single SPR response and double SPR response by based on response of absolute deferent between the first SPR resonance and the second SPR resonance of double resonance. The comparison between the results obtained and the SPR detector data in Handbook of Surface Plasmon Resonance [12] proves that we can practice this device in the field of biomedical detection.

References

[1] L. Touahir, E. Galopinb et al., Biosensors and Bioelectronics **25**, 2579 (2010).
[2] Zongru. Zhan, Xingyi Ma et al., Biosensors and Bioelectronics **32**, 127 (2012).
[3] Y. Liu, J. Kim, Sensors and Actuators B: Chemical **148**, 23 (2010).
[4] Gerardo A. López-Muñoz et al., Biosensors and Bioelectronics **96**, 260, (2017).
[5] Subash C. B. Gopinath, Sensors and Actuators B **150**, 722 (2010).
[6] Nikolai G. Khlebtsov, Lev A. Dykman, Journal of Quantitative Spectroscopy & Radiative Transfer **111**, 1 (2010).
[7] Chii-Wann Lin, Kuo-Ping Chen et al., Optical and Quantum Electronics **37**, 1423 (2005).
[8] Tuan Vo-Dinh, Fei Yan, David L. Methods in Molecular Biology **300**(12), 255 (2005).
[9] Tomáš Riedel, František Surman et al., Biosensors and Bioelectronics **85**, 272 (2016).
[10] A. Elmholdt Christensen, C. Uhrenfeldt et al., Energy Procedia **10**, 111 (2011).
[11] Di Qu, Fang Liu, Xujie Pan et al., 37th IEEE, Plasmonic Core-Shell Nanoparticle Enhanced Optical Absorption In Thin Film Organic Solar Cells, 924 (2011).
[12] Richard B. M. Schasfoort, Handbook of Surface Plasmon Resonance 2nd Edition (Book style). Royal Society of Chemistry, 544 (2017).
[13] D. Courjon, C. Bainier, Le champ proche optique théorie et applications, SpringerVerlag France, (2001).
[14] E. Thomas, Furtak Miles, V, Klein, Optics (Book style). wely, 2eme edition, 676 (1986).
[15] J. Singh, Optical Properties of Condensed Matter and Applications (Book style), edition Wiley & Sons, 440 (2006).
[16] E. Sternberg el al., Journal of Colloid and Interface Science **143**(2), 513 (1991).